Nanomed Res J 9(4):381-392, Autumn 2024

RESEARCH ARTICLE

Chitosan-coated PDMS sponge supported Zn-MOFs: fabrication, characterization and assessment of their biocompatibility and antibacterial activity

Zeinab Ansari-Asl[1,*], Zahra Shahvali[1], Reza Sacourbaravi[1], Esmaeil Darabpour[2], Elham Hoveizi[2]

[1] *Department of Chemistry, Faculty of Science, Shahid Chamran University of Ahvaz, Ahvaz, Iran*

[2] *Department of Biology, Faculty of Science, Shahid Chamran University of Ahvaz, Ahvaz, Iran*

ARTICLE INFO

Article History:
Received 24 Jul 2024
Accepted 21 Nov 2024
Published 01 Dec 2024

Keywords:
Metal-organic framework
Polydimethylsiloxane
Chitosan
Biocompatibility
Antibacterial Activity

ABSTRACT

Nanocomposite sponges composed of biocompatible polymers and inorganic materials have attracted much attention within various fields such as biomedicine, pharmaceutics, and food packaging. In this study, we have fabricated some novel nanocomposites with a combination of salt leaching for fabrication of PDMS (polydimethylsiloxane) sponge, *in situ* synthesis of Zn-based metal-organic framework (Zn-MOF), and dip coating process for coating Zn-MOF@PDMS sponge with chitosan. Chitosan stabilizes Zn-MOF particles and promotes the biocompatibility of the as-obtained composites. The surface morphology of PDMS and its nanocomposites was investigated by scanning electron microscope (SEM). X-ray diffraction was conducted to study the microstructure of the prepared Chitosan@Zn-MOF@PDMS sponge. The nanocomposite sponge, Chitosan@Zn-MOF@PDMS, was also studied by elemental EDS mapping technique. The antibacterial and cytotoxicity activities of the as-prepared sponges were also evaluated. Chitosan and Zn-MOF improved the antibacterial properties of the PDMS sponges against *Escherichia coli* and *Staphylococcus aureus*. The Chitosan@Zn-MOF@PDMS sponge exhibited a remarkable decline in the amount of viable bacteria cells (> 4.5 log10 CFU). The obtained Biological results showed that the as-obtained scaffolds, Zn-MOF@PDMS and Chitosan@Zn-MOF@PDMS, had suitable surfaces for attachment of cells and proliferation compared to the pure PDMS scaffold. The Chitosan@Zn-MOF@PDMS sponge has the potential for antibacterial and tissue engineering purposes owing to their biocompatibility, porosity, and good mechanical stability.

How to cite this article
Ansari-Asl Z., Shahvali Z., Sacourbaravi R., Darabpour E., Hoveizi E. Chitosan-coated PDMS sponge supported Zn-MOFs: fabrication, characterization and assessment of their biocompatibility and antibacterial activity. Nanomed Res J, 2024; 9(4): 381-392. DOI: 10.22034/nmrj.2024.04.005

INTRODUCTION

A scaffold is considered a critical component in the tissue engineering (TE) field owing to providing proper support for cell adhesion and growth. These structures are in contact with tissue after implantation, so, a suitable scaffold should have biocompatibility, bio-stability, and also proper surface properties including roughness and morphology [1, 2]. Various natural and synthetic materials such as metals, polymers, and composites have been used for the preparation of tissue engineering scaffolds [3, 4].

Owing to the importance of porosity in tissue engineering, the fabrication of polymeric micrometer-, nanometer-sized porous structures (sponges) has been considerably researched. Synthetic biocompatible polymers such as polydimethylsiloxane (PDMS) have been used as scaffolds due to their superior biodegradability and biocompatibility, low cost, and excellent mechanical properties [5, 6]. However, the application of pure PDMS is limited in TE due to its hydrophobicity. Therefore, to solve this problem, increasing the hydrophilicity of PDMS sponges is needed. Incorporating hydrophilic MOFs into the PDMS

* Corresponding Author Email: *z.ansari@scu.ac.ir*

matrix can be used to improve the hydrophilicity of PDMS, porosity as well as roughness [7, 8].

MOFs are versatile porous materials synthesized from metal ions and organic linkers. Owing to their many advantages consisting of regular pores, ultrahigh porosity, as well as chemical stability, MOFs have served as excellent materials for some applications such as gas storage, catalysis, sensing, molecular separation, diagnostics, and therapeutics in biomedicine [9-11]. The application of MOFs in the biological fields, however, is restricted due to their low mechanical properties and particle forms. Fabrication of nanocomposites of MOFs with biocompatible polymers such as chitosan, cellulose, PCL (poly(ε-caprolactone), polylactic-co-glycolic acid, and PLA (polyLactic Acid) can be used to overcome these shortcomings [12-15].

Postoperative infection due to the bacteria adhesion into scaffolds can be prevented using antibacterial agents such as chitosan. The antibacterial property of chitosan was widely investigated and used in recent years. Chitosan owing to its biocompatibility, biodegradability, and nontoxicity exhibits more advantages in comparison to inorganic antibacterial agents such as Ag nanoparticles [16, 17]. This material is a natural polysaccharide that shows intrinsic antibacterial and good adhesion activity and can induce proliferation, differentiation, and cell adhesion. Furthermore, the $-NH_2$ and OH moieties, polar groups, in the chitosan structure can enhance the hydrophilic character of the final composites [18, 19].

Generally, it seems that the incorporation of Zn-MOF as an additive into PDMS and coating with hydrophilic chitosan has a synergetic effect on biocompatibility and antibacterial activity. This research aimed to develop PDMS sponges using salt leaching, followed by the incorporation of Zn-MOFs to obtain functional composite materials. Finally, some new Chitosan@Zn-MOF@PDMS nanocomposite sponge was coated with chitosan by the dip-coating procedure. The antibacterial activity of the nanocomposite sponges was studied against *Escherichia coli* and *Staphylococcus aureus*. Additionally, some biological studies including cell viability and cell proliferation were also conducted.

EXPERIMENTAL

Materials and methods

Zinc(II) acetate hexahydrate, ethanol, chitosan, PDMS, citric acid, and acetic acid were purchased from Merck Company. 1, 3, 5-benzenetricarboxylic acid were supplied from Sigma Aldrich Company. FTIR spectra of the fabricated compounds were obtained using an FT BOMEM MB102 spectrophotometer. The microstructure of the as-prepared materials was characterized using the X-ray diffraction technique (XRD, X'Pert Pro using CuKα radiation). The morphological properties of the sponges were investigated with TESCAN MIRA3 and *KYKY-EM3200* Scanning Electron Microscope (SEM).

Synthesis of Zn-MOF

Zn-MOF was synthesized by the method described in the reported reference [20]. In brief, a solution of 14.30 mmol (3.13 g) of $Zn(OAc)_2.6H_2O$ in 25 mL of H_2O was mixed with a 9.50 mmol (2.00 g) of 1,3,5-benzenetricarboxylic acid, in 25 mL of EtOH. The obtained solution was sonicated for 90 min. The product was centrifuged, ethanol-washed, and subsequently dried at 60 °C for 24 h to ensure purity and optimal processing conditions.

Fabrication of PDMS sponges

The PDMS prepolymer and thermal curing agent were mixed with a 10:1 ratio. Then, citric acid monohydrate was added to the PDMS (1:1 or 3:1 mass ratios) and the obtained mixture was stirred magnetically for 1 h, and then cured for 2 h at 80 °C to conduct polymerization. Finally, the as-fabricated 3D PDMS sponge was kept in EtOH under mild shaking for 24 h to remove citric acid; EtOH was changed several times. The PDMS (1:1) and PDMS (1:3) sponges were prepared after drying.

Fabrication of Zn-MOF@PDMS sponge

To obtain a Zn^{2+}@PDMS sponge, an aqueous solution of zinc nitrate was prepared by dissolving 0.63 g of $Zn(NO_3)_2.6H_2O$ in 15 mL EtOH. The fabricated PDMS sponge was submerged in the solution and subjected to continuous agitation for 24 h to facilitate effective material interaction and modification. Then, the Zn^{2+}@PDMS sponge was separated, added into a solution of H_3BTC (0.2 g in 15 mL EtOH), and stirred for 24 h. After the modification, the Zn-MOF@PDMS sponge was isolated and dried at 60 °C for 24 h to achieve a stable composite. An identical preparation method was used to fabricate all of the Zn-MOF@PDMS composites.

Preparation of Chitosan@Zn-MOFs@PDMS sponge

The dip-coating procedure was used for the fabrication of Chitosan@Zn-MOF@PDMS sponges. 0.14 g chitosan was dissolved in 10 mL acetic acid (2%). After obtaining a bubbles free and clear solution of CS, the Zn-MOF@PDMS sponge was immersed into the prepared chitosan solution for 1 h under mild shaking. Then, the Chitosan@Zn-MOFs@PDMS sponge was separated and dried at 60 °C for 24 h.

Antibacterial activity test

Antibacterial activity of the prepared sponges was assessed against *Staphylococcus aureus* ATCC 6538 (Gram-positive) and *Escherichia coli* ATCC 25922 (Gram-negative). To investigate the antibacterial effect of sponges, bacterial suspensions, adjusted to a turbidity of 0.5 McFarland standard (1.5×10^8 CFU mL^{-1}), were prepared in saline. Sponge samples (2.5 cm^2) were then introduced to the bacterial suspensions and incubated at 37 °C with shaking (170 rpm) for 4 h. The number of CFUs was subsequently determined. To assess the long-term antibacterial effects, four cycles of evaluation were conducted, with sponge samples being washed, sterilized, and reused for each cycle.

Isolation and culture of human endometrial mesenchymal stem cells (EnMSCs)

Endometrial tissue samples were received and washed in PBS with 3% penicillin/streptomycin. After removing platelets and cutting the tissue, collagenase type 1 was applied at 1 mg mL^{-1} for 2 h to facilitate enzymatic processing. The processed tissue was passed through a 70 µm strainer, and the resulting cells were cultured in a DMEM/F12 medium supplemented with 10% FBS and 1% pen/strep to promote cell growth and proliferation.

Seeding of human endometrial mesenchymal stem cells on the scaffolds

Before culturing EnMSCs on the scaffolds, the scaffolds were immersed in 70 °C ethanol for 5 minutes and then immersed in sterile PBS for 24 h. For further sterilization, the scaffolds were revealed to UV light for 4 h. Then, the scaffolds were punched into discs with a diameter of 6 mm and embedded in 96-plate plates, and 1×10^4 cells/well was seeded to each disc.

Preparation of samples for scanning electron microscopy (SEM)

For SEM photography, the EnMSCs were seeded on PDMS scaffolds and cultured for 3 days. Then for SEM photography, the culture media was carefully withdrawn from wells and the cells were washed with PBS and fixed with 300 µL of 2.5% glutaraldehyde solution (Sigma, USA) and maintained at 25 °C for 2-3 h. Ascending concentrations of ethanol (30, 50, 60, 70, 80, 90, and 100%) were used for the dehydration step. Then, the photos were taken after covering the samples with gold utilizing an SEM microscope (LEO 1455VP, Japan).

The cell viability analysis

Shortly, EnMSCs were seeded on PDMS scaffolds with a number of 1×10^4 cells/scaffold. The samples were cultured in DMEM/F12 media supplementary with 10% FBS for cell attachment, penetration, and growth on the scaffolds. Then, after 1-3 days, cell viability was evaluated by MTT solution with a concentration of 0.5 mg mL^{-1}. After 3-4 h the supernatant solutions were withdrawn and 100 µL of DMSO was added to each well for dissolution of the formazan. The absorbance was measured at 570 nm by an ELISA reader (Fax STAT, USA). In this examination, 2D culture was assessed as a control sampling.

Acridine Orange/ Ethidium Bromide staining

In this process, EnMSCs were first seeded on the PDMS scaffolds for 48 h in DMEM/F12 media supplemented with 10% FBS. Cells were then fixed with 4% paraformaldehyde for 30 min. The cells were then washed with PBS and the acridine orange/ethidium bromide solution (100 µg mL^{-1}) was added in each well for 5 min. After that, the samples were obeyed and photted with a fluorescent microscope (Olympus, Japan).

RESULTS AND DISCUSSION

Preparation and characterization of materials

Chitosan@Zn-MOF@PDMS nanocomposite was successfully fabricated by a three-step process consisting of salt leaching, *in situ* synthesis of Zn-MOFs, and dip-coating processes. Scheme **1** shows the procedure of composite fabrication in detail. The PDMS pre-polymer and curing agent were mixed with citric acid particles and then cured at 80°C. After the leaching of citric acid particles by dissolving in ethanol, PDMS sponges were created. Then, Zn-MOF was incorporated into the PDMS sponge. The PDMS and Zn-MOF@PDMS sponges were coated with a thin layer of chitosan using the

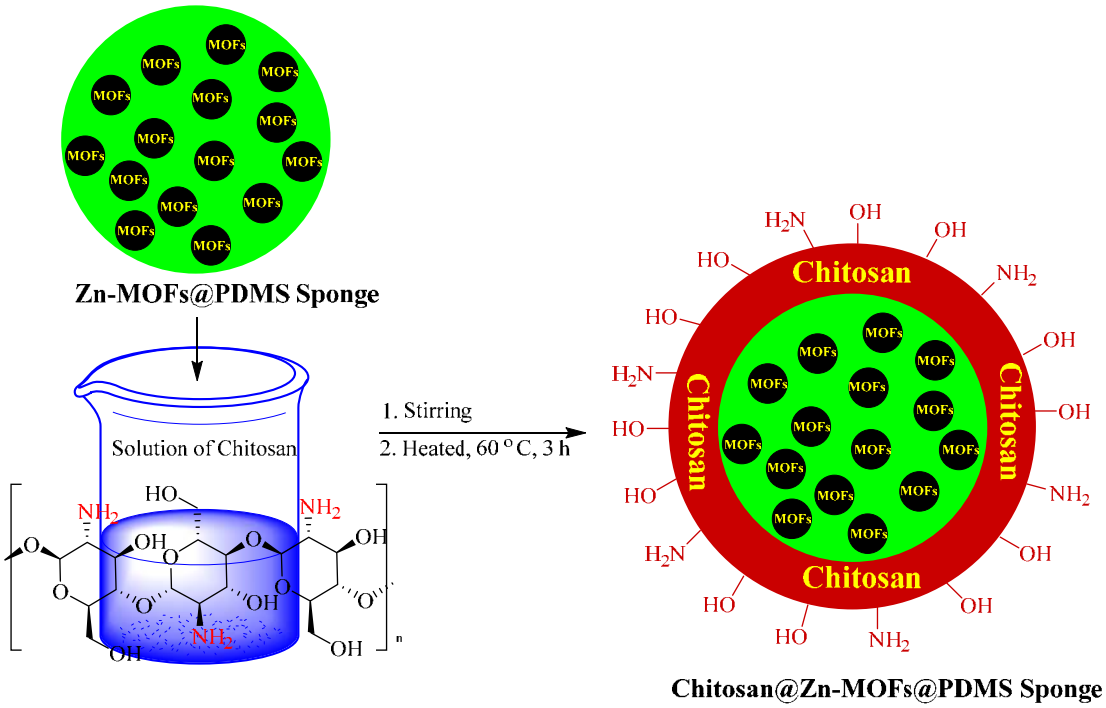

Scheme 1. Fabrication of PDMS incorporated by Zn-MOF and coated with chitosan.

dip-coating method. The structural characterization of the nanocomposites was investigated using FT-IR, XRD, SEM, and EDS mapping techniques.

Figure **1** illustrates the FT-IR spectra of the as-prepared compounds. The incorporation of Zn-MOF into the PDMS was confirmed by comparison of the IR spectrum of the PDMS, Zn-MOF, and the nanocomposites. The Zn-MOF showed a band at 741 cm^{-1} that is characteristic of Zn-O groups. The absorption band at 1439, 1556, and 1618 corresponded to the C-C, C-O, and C=O bond vibrations, respectively [22, 23]. For PDMS, the ν(Si-C-H), ν(Si-O), ν(Si-C), and ν_{asym}(C-H) are observed at 805, 1024, 1258, and 2960 cm^{-1}, respectively [24, 25]. Additionally, the Chitosan@Zn-MOF@PDMS sponge showed absorption peaks that are related to the coated chitosan. The chitosan has characteristic bands at 1398, 1423, 1578, and 1632 cm^{-1} which can be related to the CH_2-OH, CH-OH, N-H, and C=O, respectively [26, 27].

X-ray diffraction analysis was employed to examine the crystallinity and structural properties of the fabricated materials. The XRD patterns of Zn-MOF, PDMS, Zn-MOF@PDMS, and Chitosan@Zn-MOF@PDMS are presented in Figure **2**. The PXRD pattern of Zn-MOF exhibits strong peaks at 2θ = 18.67°, 19.43°, 22.19°, corresponding to (331), (420), and (333) Planes, respectively [22]. The PDMS displays broad diffraction peaks at 12° and 22.5° which confirm its amorphous nature [28]. The diffraction peaks of the Zn-MOF disappear in the Zn-MOF@PDMS and Chitosan@Zn-MOF@PDMS which can be corresponded to lower percent and homogeneous dispersion of the Zn-MOF in the PDMS matrix.

SEM technique was applied for studying the morphological feature of PDMS and its composite sponges (Figure **3**). SEM images of PDMS, Zn-MOF@PDMS, and Chitosan@Zn-MOF@PDMS sponges demonstrate that the PDMS sponge's morphology remains consistent upon incorporation of Zn-MOFs and chitosan into the polymer matrix, indicating that the combination process does not significantly alter the sponge's structure. Additionally, SEM images of the Zn-MOF@PDMS showed that the Zn-MOF nanoparticles were firmly incorporated into the holes and surface of PDMS sponges.

Si, Zn, and N elemental EDS mapping for the Chitosan@Zn-MOF@PDMS are shown in Figure **4**. The EDS-mapping also approves the incorporation of Zn-MOF and chitosan into the surface of the PDMS sponges.

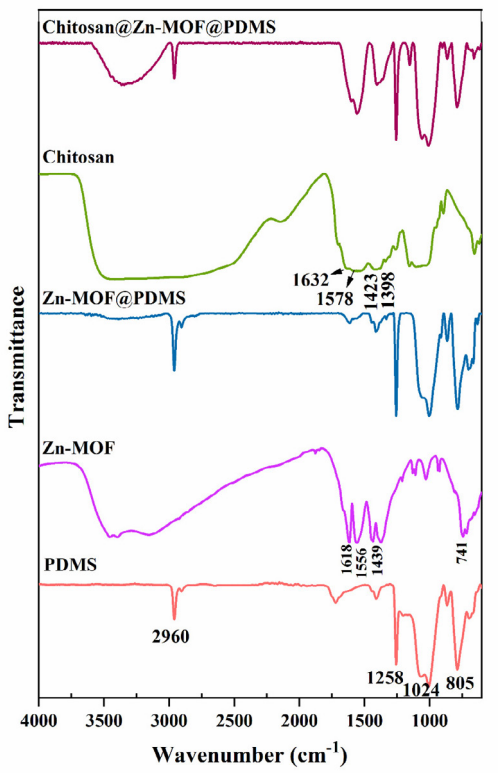

Fig. 1. FT-IR spectra of Zn-MOF, PDMS, Zn-MOF@PDMS, and Chitosan@ Zn-MOF@PDMS.

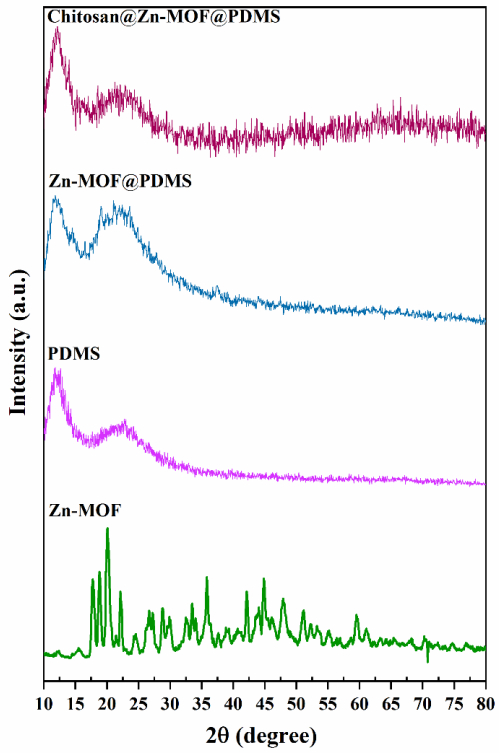

Fig. 2. XRD patterns of Zn-MOF, PDMS, Zn-MOF@PDMS, and Chitosan@ Zn-MOF@PDMS.

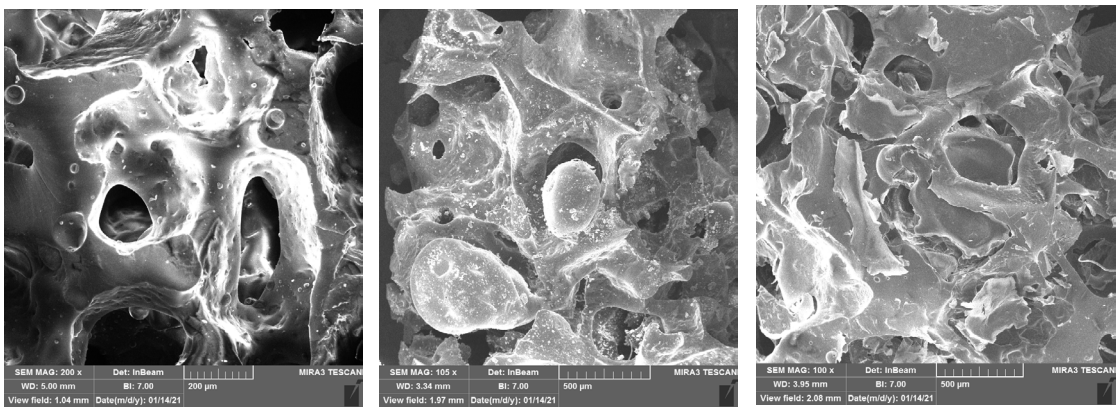

Fig. 3. SEM images of (a) PDMS, (b) Zn-MOF@PDMS, and (c) Chitosan@Zn-MOF@PDMS.

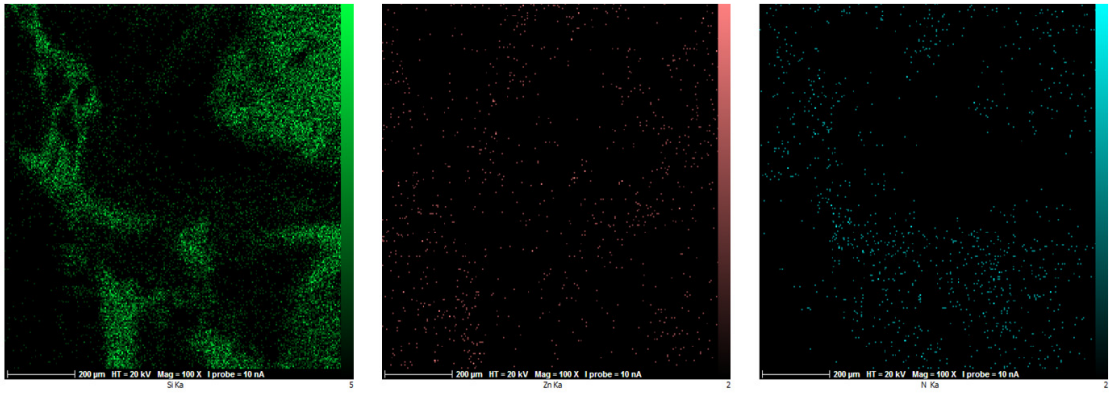

Fig. 4. Si, Zn, and N elemental mapping of Chitosan@Zn-MOF@PDMS.

Antibacterial activity of the as-prepared sponges

In this study, bactericidal (lethal) action was defined as the treatment that resulted in a ≥ 3 $\log_{10}$ reduction in CFU. The results, which are presented in Figures **5** and **6**, showed that the activated sponges were effective against both gram-negative and gram-positive bacteria used in this study. The PDMS-chitosan film caused less than 2 $\log_{10}$ CFU reduction in the number of viable bacteria. The results showed the addition of Zn-MOF to the PDMS sponges, potentiated the antibacterial activity against *tested* bacteria. The lethal effect on *E. coli* cells was observed by the use of Zn-MOF@PDMS (3:1) and Chitosan@Zn-MOF@PDMS (3:1) sponges. The bactericidal activity against *S.aureus* was achieved by the use of Zn-MOF@PDMS (3:1), Chitosan@Zn-MOF@PDMS (1:1), and Chitosan@Zn-MOF@PDMS (1:3) sponges. The PDMS sponges containing Zn-MOF induced concentration-dependent decreases in cell viability. The Zn-MOF has a good antibacterial effect by releasing Zn^{2+} to kill microorganisms [29]. In this study, the combination of chitosan and Zn-MOF showed synergistic antibacterial activity against tested bacteria in which chitosan likely enhanced the penetration of Zn^{2+} ions into the cell by its membrane-damaging ability [30]. Also, it was found that the antibacterial activity of the activated composites could be conserved even after rinsing four times, suggesting their potential use in long-term antibacterial coatings.

Biological studies of the as-obtained scaffolds

Morphology of human endometrial mesenchymal stem cells

The morphology of the extracted EnMSCs is shown in Figure **7**. As shown in figure **7a**, EnMSCs could adhere to the bottom of the flask on the

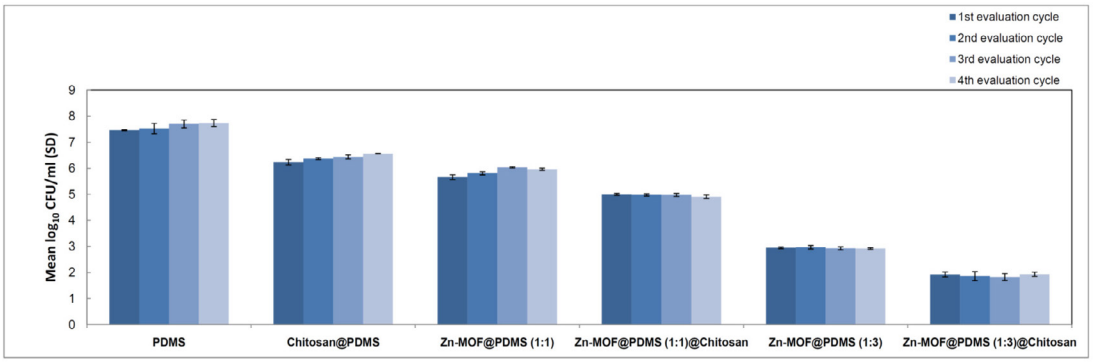

Fig. 5. Antibacterial effect of Chitosan@PDMS, Zn-MOF@PDMS, and Chitosan@Zn-MOF@PDMS composites against *E. coli* after different washing cycles.

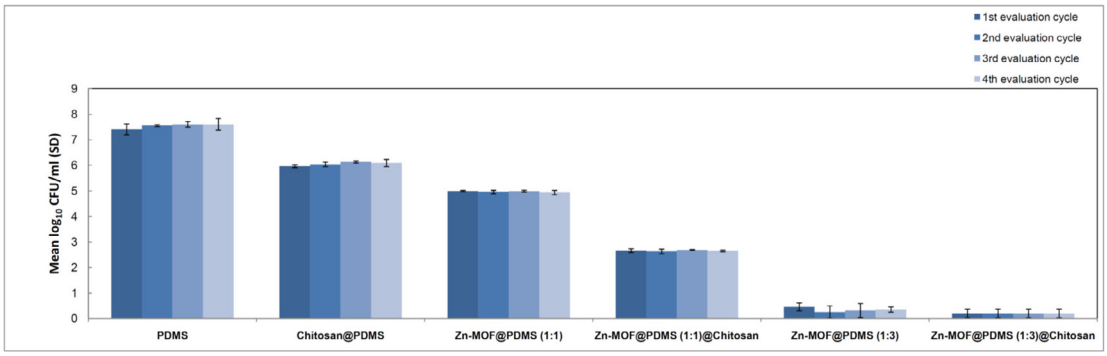

Fig. 6. Antibacterial effect of Chitosan@PDMS, Zn-MOF@PDMS, and Chitosan@Zn-MOF@PDMS composites against *S. aureus* after different washing cycles.

first day after isolation with low density. Figure **7b** exhibits the EnMSCs in the third passage. The cells are homogenous and uniform with the morphology of mesenchymal cells. Here the cells are in high density and observed in a spindle shape [31, 32]. Also, the cells were in the exponential phase of growth and proliferated rapidly (Figure **7**).

Comparison of survival rate of the cells by MTT assay

Two scaffold types, with and without chitosan, were employed in this study (Figure **8**). Scaffolds coated with chitosan exhibited significantly enhanced attachment, survival, and proliferation of EnMSCs compared to those without chitosan. Additionally, among the PDMS (1:3) and PDMS (1:1) scaffolds, EnMSC attachment, survival, and proliferation were notably higher in the PDMS (1:3) scaffolds. The results also demonstrated that the presence of Zn-MOF led to substantial improvements in EnMSC attachment, survival, proliferation, and biocompatibility. Overall, chitosan-coated and Zn-MOF-containing scaffolds showed superior performance in promoting EnMSC growth. In addition, the results showed that cell survival in the cultured samples after three days was significantly higher than one day so this growth increased significantly in the samples having chitosan and Zn-MOF [33, 34]. The study's findings indicate a significant enhancement in scaffold biocompatibility when incorporating chitosan and Zn-MOFs. The comparative results between various scaffold compositions reveal that certain structural properties directly influence cellular responses. For instance, the observation that PDMS (1:3) scaffolds support higher cell survival and proliferation than PDMS (1:1) and that the presence of Zn-MOF promotes superior attachment of EnMSCs is crucial. Pella et al. explored the biocompatibility of chitosan hydrogels when used as scaffolds for cell culture. They highlight chitosan's ability to promote cell adhesion and proliferation through its favorable

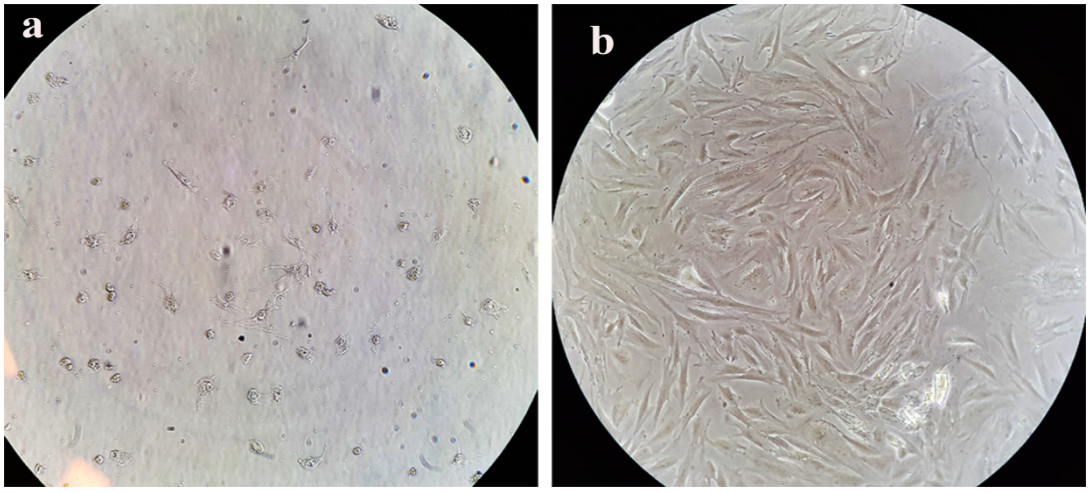

Fig. 7. The morphology of the extracted EnMSCs (20 X magnification). a) EnMSCs in the first passage. b) EnMSCs in the third passage.

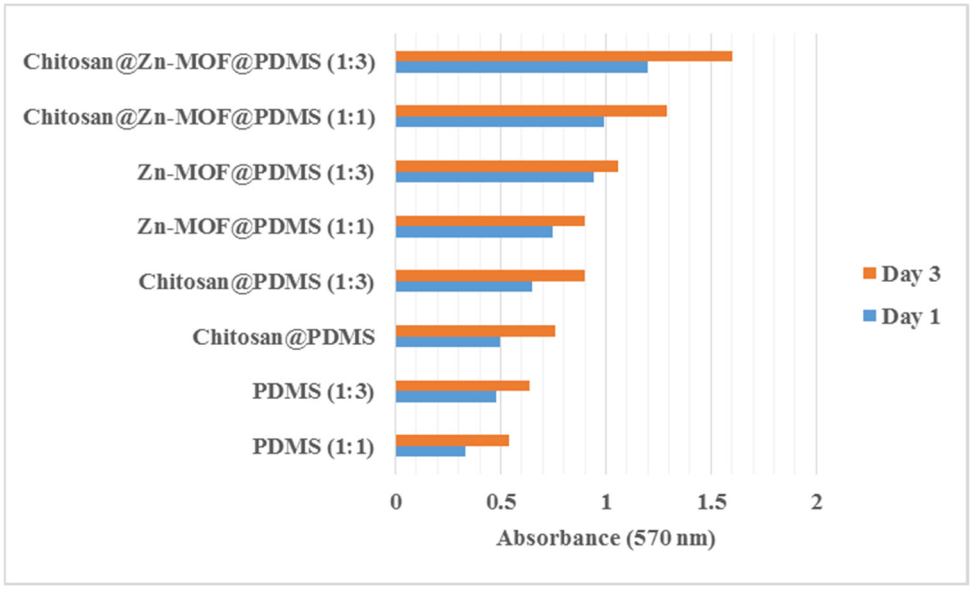

Fig. 8. Diagram of cell survival and biocompatibility of different samples by the MTT method on EnMSCs at 1 and 3 days after culture (experiments repeated three times).

chemical properties and hydrophilicity, facilitating nutrient exchange and metabolic activity. Similar to our research, they discussed MTT assays to evaluate cell viability [35]. Consistent with our study, Bahrani et al. highlighted the potential of zinc-MOFs as innovative materials in biomedicine. Their study aimed to evaluate the biocompatibility, biodegradability, and multifunctionality of these MOFs, emphasizing their applications in drug delivery, imaging, and antibacterial therapies. The findings indicate that zinc-based MOFs possess advantageous properties, including low toxicity, the ability to degrade in physiological environments, and effective encapsulation and release of therapeutic agents. The review concludes that these materials present significant promise for advancing biomedical technologies while ensuring safety and sustainability [36].

SEM investigations of cell-scaffold interactions

Figure **9** illustrates the attachment and extension of EnMSCs on the scaffolds. As shown

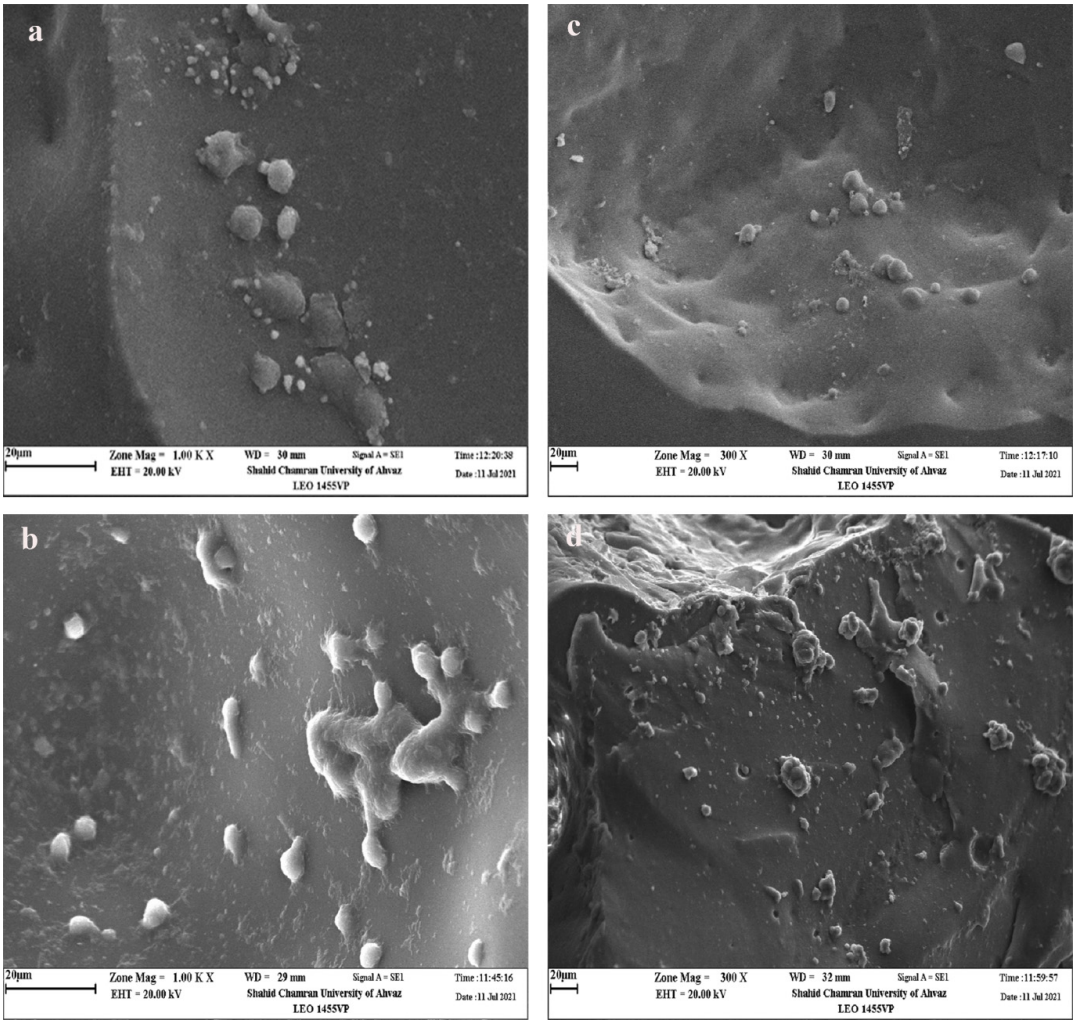

Fig. 9. SEM photographs of the interaction of EnMSCs with different samples 48 h after culture. (a) Chitosan@Zn-MOF@PDMS (1:1), (b) Chitosan@Zn-MOF@PDMS (1:3), (c) Chitosan@PDMS (1:1), and (d) Chitosan@PDMS (1:3) sponge.

in Figure **9**, the most presence of EnMSCs was related to samples **a** and **b** which contain Zn-MOF. Figures **9c** and **9d** display the Zn-MOF@PDMS sponge in the absence of Zn-MOF. Notably, sample b exhibited a significantly higher quantity of EnMSCs compared to the other samples. The permeability of Zn-MOF in PDMS (1:3) sponge is better than PDMS (1:1), because it is spongier, and the pores in it are more and larger [37]. It has also been determined that the presence of Zn-MOF increases the survival and proliferation of cells on the scaffold, so as expected, the attachment and survival of EnMSCs in the PDMS (1:3) samples were significantly higher than in the PDMS (1:1) samples [8]. The interplay between pore size and cellular infiltration in PDMS scaffolds elucidates the importance of scaffold design in tissue engineering. Larger and more interconnected pores, found in the PDMS (1:3) scaffolds, likely allow for improved oxygen and nutrient diffusion, crucial for maintaining cell viability over time. It parallels research by other authors, emphasizing that scaffold architecture is pivotal for optimizing cell-scaffold interactions [38]. Furthermore, the incorporation of Zn-MOFs not only improves biocompatibility but could also impart antibacterial properties, which is vital in preventing infection in tissue engineering applications. The increased surface area and porosity the Zn-MOFs provide may enhance the material's interactions with cells

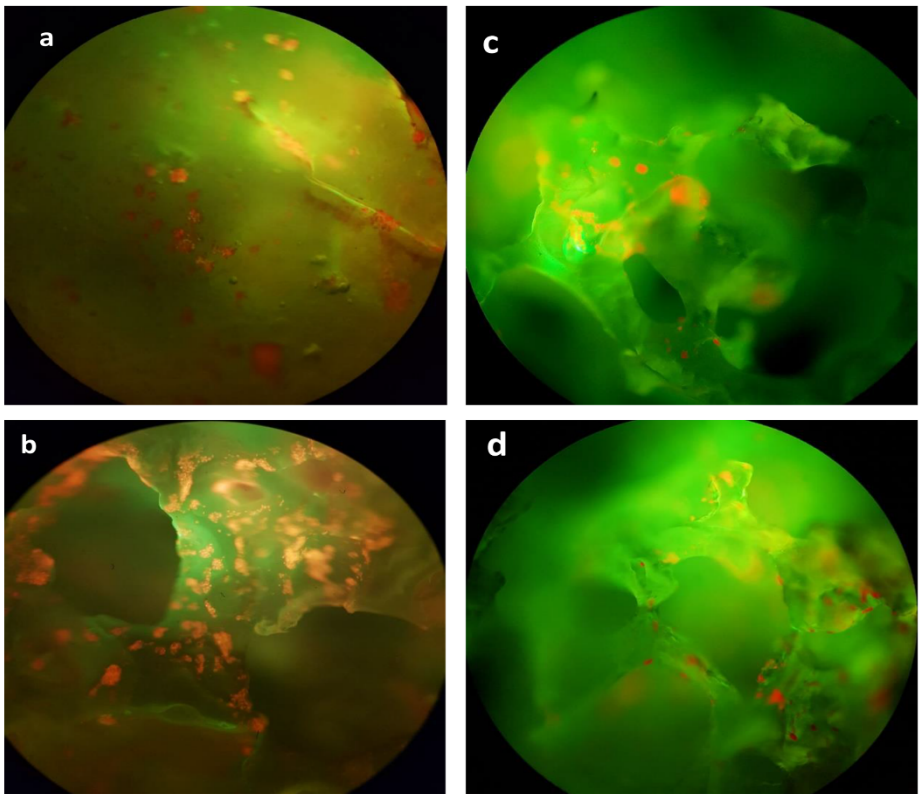

Fig. 10. Staining of the EnMSCs cultured on the different scaffolds with Acridine Orange/ Ethidium Bromide (10 X magnification). (a) Chitosan@Zn-MOF@PDMS (1:1), (b) Chitosan@Zn-MOF@PDMS (1:3), (c) Chitosan@PDMS (1:1), and (d) Chitosan@PDMS (1:3) Sponge.

and the biological environment, a trend seen in other nano-enabled composites [36]. Nalbach *et al.* synthesis and characterization of PDMS/ZnO nanocomposite scaffolds for tissue engineering. This study investigates PDMS incorporated with zinc oxide nanoparticles, discussing their effects on cell behavior and antibacterial properties. The findings show improved mechanical strength and bioactivity, reflecting results similar to Zn-MOFs in our research, where incorporating metal frameworks increases cell attachment and viability [39].

Acridine Orange/ Ethidium Bromide staining

At this stage of the research, the cells were cultured on the scaffolds for 48 h and stained with acridine orange. Acridine orange staining is double staining that is used to investigate cell death and survival. In cells stained with acridine orange, orange and red colors indicate dead cells and green color indicates living cells [40]. In this stage, because we fixed the cells, so the cells are orange in color (in the usual dyeing, because the scaffold also turns green, there was not enough contrast for the cells). Here the purpose was to check the presence of cells on scaffolds and compare their number in different samples. The results showed that the number of cells in the samples containing Zn-MOF was higher than in the samples without Zn-MOF and in the image of the Chitosan@Zn-MOF@PDMS (1:3) sponge sample, the density of cells was higher than in other samples (Figure **10**). The methodology employed, particularly using Acridine Orange staining for assessing living cell populations in various scaffold environments, supports the robust characterization of cell responses to biomaterials. This critical evaluation through quantitative assays like the MTT assay also suggests that the growth-promoting effects observed are not just qualitative; they offer a pathway for future applications in regenerative medicine. The findings of the original article align with broader research

themes in tissue engineering, shedding light on the intricate balance between material composition, scaffold architecture, and biological outcomes. Further exploration could include *in vivo* studies to validate these promising in vitro results and to assess the long-term functionality and safety of these chitosan-coated Zn-MOF scaffolds in clinical applications.

CONCLUSIONS

In this study, we have composed Zn-MOFs and chitosan with biocompatible PDMS to enhance porosity, hydrophobicity, and antibacterial activity. The Chitosan@Zn-MOF@PDMS nanocomposites combine the benefits of PDMS (flexibility, low cost, and stability), Zn-MOFs (porosity and hydrophilicity), and the antibacterial property of chitosan. The successful incorporation of the Zn-MOFs nanoparticles and chitosan into the PDMS was confirmed by FT-IR, XRD, SEM, and EDS techniques. The uniform dispersion of Zn-MOFs nanoparticles into the PDMS matrix was investigated by SEM and EDS-mapping techniques. The Chitosan@Zn-MOF@PDMS exhibit proficient antibacterial properties toward both gram-positive *S. aureus* and gram-negative bacterium *E.coil*. The obtained Chitosan@Zn-MOF@PDMS demonstrated favorable morphological and biochemical characteristics, resulting in satisfactory cell adhesion and proliferation outcomes. Therefore, the Chitosan@Zn-MOF@PDMS sponge with improved antibacterial activity and suitable biocompatibility could be used as a new environmentally friendly scaffold in the tissue engineering field.

ACKNOWLEDGMENTS

We sincerely acknowledge the Shahid Chamran University of Ahvaz for financial support (Grant No.: SCU.SC1400.29011).

DECLARATION OF INTEREST

None

REFERENCES

1. Zielińska A, et al. Scaffolds for drug delivery and tissue engineering: The role of genetics. J Control Release. 2023;359:207-23. https://doi.org/10.1016/j.jconrel.2023.05.042
2. Suhag D, Kaushik S, Taxak VB. Scaffold Design in Tissue Engineering. In: Handbook of Biomaterials for Medical Applications, Volume 1: Fundamentals. Springer; 2024:155-84. https://doi.org/10.1007/978-981-97-4818-1_6
3. Atari M, Labbaf S, Javanmard SH. The Role of Poly-glycerol Sebacate/Gelatin Coating Layer on Biological Features and Calcification Rate of 3D Melt-Molded Antibacterial Scaffold for Heart Valve Tissue Engineering. J Polym Environ. 2024;32:111-32. https://doi.org/10.1007/s10924-023-02957-0
4. Wekwejt M, et al. Hyaluronic acid/tannic acid films for wound healing application. Int J Biol Macromol. 2024;254:128101. https://doi.org/10.1016/j.ijbiomac.2023.128101
5. Miranda I, et al. Properties and Applications of PDMS for Biomedical Engineering: A Review. J Funct Biomater. 2021;13(1):[article number]. https://doi.org/10.3390/jfb13010002
6. Fortună ME, et al. Synthesis and Properties of Modified Biodegradable Polymers Based on Caprolactone. Polymers. 2023;15:4731. https://doi.org/10.3390/polym15244731
7. Zhao J, et al. MOF@Polydopamine-incorporated membrane with high permeability and mechanical property for efficient fouling-resistant and oil/water separation. Environ Res. 2023;236:116685. https://doi.org/10.1016/j.envres.2023.116685
8. Nikpour S, et al. Curcumin-loaded Fe-MOF/PDMS porous scaffold: Fabrication, characterization, and biocompatibility assessment. J Ind Eng Chem. 2022;110:188-97. https://doi.org/10.1016/j.jiec.2022.02.052
9. Zhang Y, et al. Current research status of MOF materials for catalysis applications. Mol Catal. 2024;555:113851. https://doi.org/10.1016/j.mcat.2024.113851
10. Gang SQ, et al. A stable Zr(IV)-MOF for efficient removal of trace SO2 from flue gas in dry and humid conditions. J Hazard Mater. 2024;470:134180. https://doi.org/10.1016/j.jhazmat.2024.134180
11. Deng Y, et al. Prospects, advances and biological applications of MOF-based platform for the treatment of lung cancer. Biomater Sci. 2024;12:3725-44. https://doi.org/10.1039/D4BM00488D
12. Saeed T, et al. Synthesis of chitosan composite of metal-organic framework for the adsorption of dyes; kinetic and thermodynamic approach. J Hazard Mater. 2022;427:127902. https://doi.org/10.1016/j.jhazmat.2021.127902
13. Abdelhamid HN, Mathew AP. Cellulose-metal organic frameworks (CelloMOFs) hybrid materials and their multifaceted Applications: A review. Coord Chem Rev. 2022;451:214263. https://doi.org/10.1016/j.ccr.2021.214263
14. Ramezani MR, et al. Fabrication and Characterization of Fe(III) Metal-organic Frameworks Incorporating Polycaprolactone Nanofibers: Potential Scaffolds for Tissue Engineering. Fibers Polym. 2020;21:1013-22. https://doi.org/10.1007/s12221-020-9523-6
15. Wang X, et al. The flammability and mechanical properties of poly(lactic acid) composites containing Ni-MOF nanosheets with polyhydroxy groups. Compos Part B Eng. 2020;183:107568. https://doi.org/10.1016/j.compositesb.2019.107568
16. Perinelli DR, et al. Chitosan-based nanosystems and their exploited antimicrobial activity. Eur J Pharm Sci. 2018;117:8-20. https://doi.org/10.1016/j.ejps.2018.01.046
17. Yilmaz Atay H. Antibacterial Activity of Chitosan-Based Systems. In: Functional Chitosan. 2020:457-89. https://doi.org/10.1007/978-981-15-0263-7_15
18. Zhu Y, et al. Application Progress of Modified Chitosan and Its Composite Biomaterials for Bone Tissue Engineering. Int J Mol Sci. 2022;23:6574. https://doi.org/10.3390/ijms23126574

19. Muzzarelli RAA. Chitosan composites with inorganics, morphogenetic proteins and stem cells, for bone regeneration. Carbohydr Polym. 2011;83:1433-45. https://doi.org/10.1016/j.carbpol.2010.10.044
20. Tehrani AA, et al. Ultrasound-assisted synthesis of metal-organic framework nanorods of Zn-HKUST-1 and their templating effects for facile fabrication of zinc oxide nanorods via solid-state transformation. Inorg Chem Commun. 2015;59:41-5. https://doi.org/10.1016/j.inoche.2015.06.028
21. Moreirinha C, et al. Antioxidant and antimicrobial films based on brewers spent grain arabinoxylans, nanocellulose and feruloylated compounds for active packaging. Food Hydrocoll. 2020;108:105836. https://doi.org/10.1016/j.foodhyd.2020.105836
22. Wang X, et al. A zinc(II) benzenetricarboxylate metal organic framework with unusual adsorption properties, and its application to the preconcentration of pesticides. Microchim Acta. 2017;184:3681-7. https://doi.org/10.1007/s00604-017-2382-1
23. Wu Y, et al. Zn2(C9H3O6)(C4H5N2)(C4H6N2)3 MOF as a highly efficient catalyst for chemical fixation of CO2 into cyclic carbonates and kinetic studies. Chem Eng Res Des. 2018;140:273-82. https://doi.org/10.1016/j.cherd.2018.10.034
24. Johnson LM, et al. Elastomeric microparticles for acoustic mediated bioseparations. J Nanobiotechnology. 2013;11:22. https://doi.org/10.1186/1477-3155-11-22
25. Chen D, et al. Preparation and properties of novel polydimethylsiloxane composites using polyvinylsilsesquioxanes as reinforcing agent. Polym Degrad Stab. 2015;111:124-30. https://doi.org/10.1016/j.polymdegradstab.2014.10.026
26. Fernandes Queiroz M, et al. Does the use of chitosan contribute to oxalate kidney stone formation? Mar Drugs. 2014;13:141-58. https://doi.org/10.3390/md13010141
27. Dara PK, et al. Synthesis and biochemical characterization of silver nanoparticles grafted chitosan (Chi-Ag-NPs): in vitro studies on antioxidant and antibacterial applications. SN Appl Sci. 2020;2:665. https://doi.org/10.1007/s42452-020-2261-y
28. Ferreira P, et al. Functionalization of polydimethylsiloxane membranes to be used in the production of voice prostheses. Sci Technol Adv Mater. 2013;14:055006. https://doi.org/10.1088/1468-6996/14/5/055006
29. Yang M, et al. Recent advances in metal-organic framework-based materials for anti-staphylococcus aureus infection. Nano Res. 2022;15:6220-42. https://doi.org/10.1007/s12274-022-4302-x
30. Guarnieri A, et al. Antimicrobial properties of chitosan from different developmental stages of the bioconverter insect Hermetia illucens. Sci Rep. 2022;12:8084. https://doi.org/10.1038/s41598-022-12150-3
31. Hoveizi E, et al. Small molecules differentiate definitive endoderm from human induced pluripotent stem cells on PCL scaffold. Appl Biochem Biotechnol. 2014;173:1727-36. https://doi.org/10.1007/s12010-014-0960-9
32. Hoveizi E, Tavakol S. Therapeutic potential of human mesenchymal stem cells derived beta cell precursors on a nanofibrous scaffold: An approach to treat diabetes mellitus. J Cell Physiol. 2019;234:10196-204. https://doi.org/10.1002/jcp.27689
33. Nejadshafiee V, et al. Magnetic bio-metal-organic framework nanocomposites decorated with folic acid conjugated chitosan as a promising biocompatible targeted theranostic system for cancer treatment. Mater Sci Eng C. 2019;99:805-15. https://doi.org/10.1016/j.msec.2019.02.017
34. Sadigh-Eteghad S, et al. Effects of Levodopa loaded chitosan nanoparticles on cell viability and caspase-3 expression in PC12 neural like cells. Neurosciences. 2013;18:281-3.
35. Pellá MCG, et al. Chitosan-based hydrogels: From preparation to biomedical applications. Carbohydr Polym. 2018;196:233-45. https://doi.org/10.1016/j.carbpol.2018.05.033
36. Bahrani S, et al. Zinc-based metal-organic frameworks as nontoxic and biodegradable platforms for biomedical applications: review study. Drug Metab Rev. 2019;51:356-77. https://doi.org/10.1080/03602532.2019.1632887
37. Abbasi N, et al. Porous scaffolds for bone regeneration. J Sci Adv Mater Devices. 2020;5:1-9. https://doi.org/10.1016/j.jsamd.2020.01.007
38. Montazerian H, et al. Permeability and mechanical properties of gradient porous PDMS scaffolds fabricated by 3D-printed sacrificial templates designed with minimal surfaces. Acta Biomater. 2019;96:149-60. https://doi.org/10.1016/j.actbio.2019.06.040
39. Nalbach JR. Design and characterization of polymer nanocomposites for engineering applications. Rowan University; 2018.
40. Ciniglia C, et al. Acridine orange/Ethidium bromide double staining test: A simple In-vitro assay to detect apoptosis induced by phenolic compounds in plant cells. Allelopathy J. 2010;26:301-8.